"Pre-seeding"-assisted synthesis of a high performance polyamide-zeolite nanocomposite membrane for water purification†

Chunlong Kong,[a] Takuji Shintani[b] and Toshinori Tsuru*[a]

Received (in Montpellier, France) 24th July 2010, Accepted 28th July 2010
DOI: 10.1039/c0nj00581a

A new type of zeolite-incorporated thin polyamide nanocomposite membrane that exhibits high water flux with high solute rejection can be synthesized by "pre-seeding" modified zeolite particles on a polysulfone ultrafiltration support surface prior to interfacial polymerization.

Reclamation of pure water from non-traditional water sources has increased in importance,[1] and reverse osmosis (RO) is gaining popularity as a method for producing pure water from sea water or brackish water.[2] Current RO and nanofiltration (NF) membrane production methods (*e.g.*, interfacial polymerization) provide little control over the size of interstitial voids or "nanopores".[3] RO membranes typically consist of a polymer active layer that is dense, amorphous and thin (<0.2 μm), with interstitial voids (≤0.5 nm) between the polymer chains.[4] An unfortunate dichotomy exists: as the rejection level of polymer membranes fabricated from conventional membrane materials increases, the permeability invariably decreases, and *vice versa*.[5] To tackle this challenging issue, organic–inorganic polymer membranes that can improve separation, reaction and sorption capacity, as well as enhancing chemical and thermal stability, have attracted a wide interest.[6] For example, zeolite and carbon nanotube have been dispersed within relatively thick membrane films for high gas permeability.[7] However, there have been a limited number of attempts to fabricate organic–inorganic polymer membranes for use in water desalination.[8] Unfortunately, producing a better organic–inorganic desalination membrane has become quite a challenge, because it is hard to well-disperse inorganic materials within thin polymer membrane films without inducing defects. Thus, as higher permeability always seems to be offset by lower solute rejection, none have been reported to be able to perform high water permeability with high salt (NaCl) rejection (>95%). Although these works have been envisaged, the results remain far from satisfactory.

Here, we report a new strategy for producing a promising organic–inorganic nanocomposite membrane for use in water purification. The organic materials used were modified zeolite crystals pre-assembled on a polysulfone (PSF) ultrafiltration support that served as "seeds" for polyamide-zeolite (PZ) nanocomposite membrane fabrication. A subsequent interfacial polymerization (IP) was induced that included zeolite, which led to zeolite crystals being incorporated into the thin polyamide membrane without generating defects (pinholes or cracks). In this manner, a challenging inorganic material-incorporated thin nanocomposite membrane could be fabricated with high performance by two simple steps: "pre-seeding" and polymerization. The intrinsic and well-defined zeolite pores should serve as a short cut for water permeation (Fig. 1).[9] Well-dispersed zeolite crystals modified with the organic materials were assembled easily on a PSF support as follows. Zeolite pre-assembled PSF supports were prepared by adding a specific amount of trimesoyl chloride (TMC), hexane and ethanol solution containing well-dispersed zeolite Y crystals onto PSF supports that were impregnated with a *m*-phenylenediamine (MPD) solution, so that the assembled zeolite would be modified by the polyamide and solvent after unforced evaporation of the excess solution, which induced the following IP reaction, including zeolite.

Zeolite crystals (~250 nm) were prepared from zeolite Y microcrystals by a simple grinding method (see Fig. S1†). First, a specific amount of microcrystal zeolite powder was loaded in the grinding machine for a milling time of 3 h. Second, the milled powder was dispersed in an aqueous solution under ultrasonication for 30 min, and then the large zeolite particles were removed by centrifugation at 2000 rpm for 20 min. Third, the small zeolite crystals were recovered by centrifugation at 5000 rpm for 30 min, and then the recovered products were dried at 120 °C for 1 d. Both PZ and polyamide (PA) membranes were prepared on PSF supports. To fabricate a better PZ nanocomposite membrane (see Fig. S2†), first, a 1 mL aqueous solution of MPD (2 wt%) and sodium lauryl

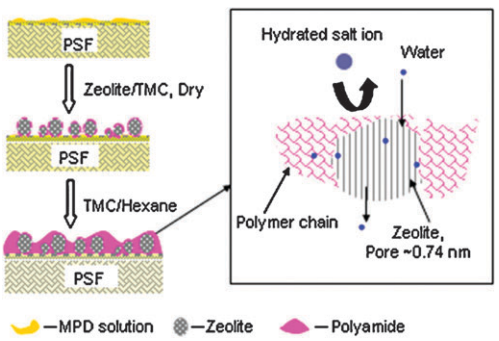

Fig. 1 A schematic representation of a PZ nanocomposite membrane fabrication and a proposed mechanism of water desalination. Reactant trimesoyl chloride (TMC) dissolved in hexane and reactant *m*-phenylenediamine (MPD) dissolved in water diffuse toward one another and react to form the polyamide membrane.

[a] *Departmentof Chemical Engineering, Hiroshima University, Higashi-Hiroshima, 739-8527, Japan. E-mail: tsuru@hiroshima-u.ac.jp; Fax: +81 824-7714; Tel: +81 824-7714*
[b] *Nitto Denko Corporation 1-1-2, Shimohozumi, Ibaraki Osaka, 567-8860, Japan*

† Electronic supplementary information (ESI) available: Further experimental details. See DOI: 10.1039/c0nj00581a

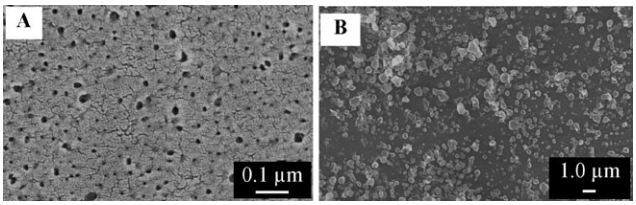

Fig. 2 FE-SEM images of the PSF support (A) and zeolite-"pre-seeded" PSF support (0.4 wt%) (B).

sulfate (0.15 wt%) was poured onto the PSF ultrafiltration membrane (diameter: 4.0 cm). The excess solution was then removed after 2 min. Second, a 0.2 mL hexane solution of TMC (0.02–0.05 wt%), zeolite (0.05–0.6 wt%) and ethanol (5–15 wt%) was uniformly coated onto the PSF support. Herein, a well-dispersed zeolite in the hexane solution was obtained with the help of adding anhydrous ethanol as a co-solvent and ultrasonication. This solution can quickly spread on the flat PSF support surface because of the positive spreading coefficient of hexane solvent.[10] After unforced evaporation of the excess solution, the solution of TMC (0.1 wt%) and hexane was immediately and mildly poured onto the "pre-seeded" support, followed by a 40–50 s polymerization reaction. Finally, the membrane was thoroughly washed with de-ionized water. The PA membrane was prepared using a conventional process without zeolite (see Fig. S3†).

The top view of the PSF ultrafiltration support was examined by scanning electron microscopy (FE-SEM) (Fig. 2A). The FE-SEM image (Fig. 2B) apparently shows that well-dispersed zeolite crystals are assembled on the PSF support, which serve as "seeds" for the following PZ nanocomposite membrane fabrication. Strikingly, the FE-SEM image (Fig. 3B) clearly shows a compact and flat surface morphology of the PZ nanocomposite membrane, whereas that of the conventional pure polyamide (PA) membrane is a uniquely characteristic "ridge-and-valley" structure (Fig. 3A).[11] In addition, the previously reported nanocomposite membranes were fabricated by adding inorganic particles into a TMC-hexane

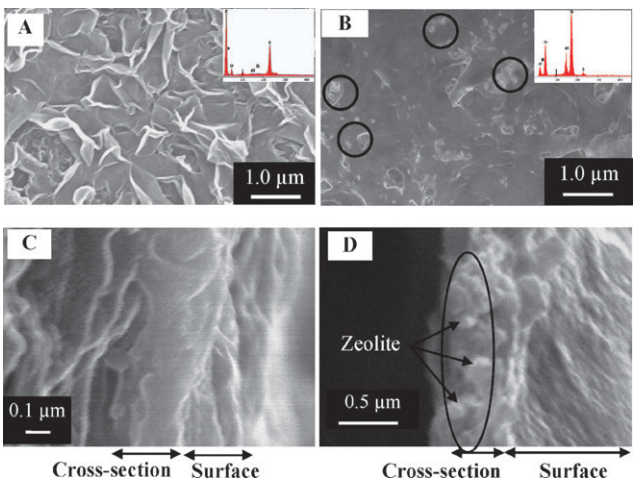

Fig. 3 FE-SEM images of the pure polyamide membrane (A, C) and PZ nanocomposite membrane (0.4 wt%) (B, D) with their energy-dispersive X-ray (EDX) spectra. (A, B) surface; (C, D) cross-section. Black circles indicate zeolites.

solution and showed a similar surface morphology to the conventional PA membrane.[12] Herein, the robust morphology of the PZ nanocomposite membrane possibly indicates that the "pre-seeded" zeolite took part in the following polymerization reaction, which led to better-dispersed zeolite within the thin polymer membrane. As Freger theoretically predicted, a narrow reaction zone appeared at the initial stage of IP.[13] The polyamide and organic solvent-modified zeolite prefers hexane to water, which induces the following IP, which includes the zeolite and results in a better zeolite-incorporated polyamide membrane. Compared with the PA membrane, EDX spectra of the PZ membrane obviously confirmed that the PZ membrane was composed of polyamide and incorporated zeolite (Si and Al). Moreover, the surface image of the PZ membrane reveals few isolated and aggregated zeolites, and the cross-section of the PZ membrane apparently indicates that the zeolites are embedded within thin polyamide membrane (Fig. 3B and D). An infrared spectrum (FT-IR) analysis of the PA membrane and the PZ nanocomposite membrane is provided in the ESI (see Fig. S4†), which shows that multiple wide peaks appear between 1200 and 1000 cm^{-1} in the PZ membrane. This is due to the presence of Si–O groups in the zeolite, which appear at almost the same frequency as C–O stretching.[14]

Table 1 shows a water permeability and rejection of 2000 ppm NaCl using the pure PA membrane and the PZ nanocomposite membrane with different zeolite content loadings. For comparison, the PZ (*) nanocomposite membranes were also fabricated by conventional methods (see Fig. S3†). The precision of the permeability and rejection measurements was estimated to be within ±10% and ±1%, respectively. As shown by Table 1, water permeability of the PZ nanocomposite membranes increased significantly with a higher zeolite loading. In addition, the rejection of NaCl in the case of the PZ membranes remained at 95–98% with a water permeability of 2.1×10^{-12} to 5.8×10^{-12} m Pa^{-1} s^{-1}. Interestingly and strikingly, the trade-off relationship between permeability and selectivity was not obvious with increased zeolite loading (less than 0.4 wt%). However, the PZ nanocomposite membranes fabricated by the conventional method showed undesirable permeability properties in this work. When the water permeability of the PZ1* membrane increased, the salt rejection decreased. It is a challenge to disperse zeolite crystals in a non-polar organic solvent such as hexane, which leads to aggregate zeolites in the solvent and can easily induce solute-permeable defects in the resultant membrane (see Fig. S5†). On the other hand, the PZ2* membrane showed approximately the same performance as the PA membrane. Although the zeolite crystals were well-dispersed in an aqueous solution, they were impregnated and covered with an adequate amount of MPD aqueous solution, which led to the following IP process to occur beyond the zeolite crystals. The resultant polyamide layer (on a zeolite layer) was similar to the pure PA membrane. The pre-assembled zeolites that were covered with the polyamide and organic solvent on the support induced the subsequent polymerization process, including zeolite, which resulted in a better zeolite-incorporated thin polyamide membrane (Fig. 3B and D).

Table 1 Permeability properties of the PA membrane and PZ nanocomposite membrane for 2000 ppm NaCl at a temperature of 298 K and a pressure of 1.5 MPa[a]

Membrane	Zeolite (wt%)	Permeability/10^{-12} m Pa^{-1} s^{-1}	Rejection (%)
PA	0	2.1	98.1
PZ1*	0.2	2.9	94.6
PZ2*	0.2	1.9	99
PZ3	0.05	3.2	97.5
PZ4	0.1	3.9	97.6
PZ5	0.2	4.2	97.4
PZ6	0.4	5.8	95.6
PZ7	0.6	6.9	87.8

[a] Membranes PZ1* and PZ2* were fabricated by the conventional method. PZ1* was prepared by adding zeolite into a TMC-hexane solution; PZ2* was prepared by adding zeolite into an MPD aqueous solution. Membranes PZ3–PZ7 were fabricated by the "pre-seeding" method.

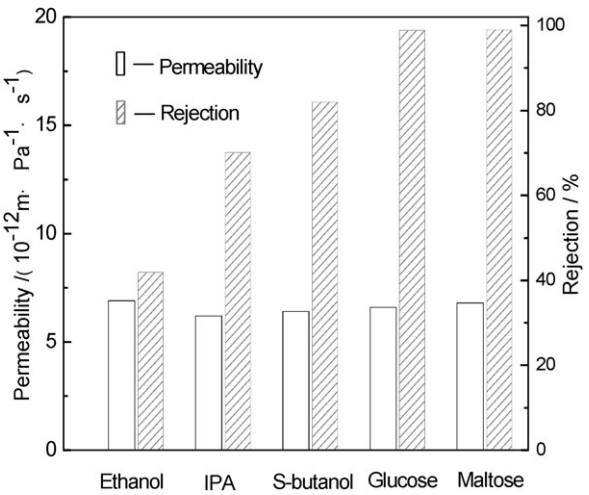

Fig. 4 Permeability properties of the PZ (0.4 wt%) membrane for a series of neutral organic solutions of different molecular sizes at a temperature of 298 K and a pressure of 1.5 MPa.

Fig. 4 shows the observed permeability and rejection rates of the five test molecules with different Stokes radii. Because the solute rejection rate for both NF and RO was determined by molecular sieving,[15] the rejection rates for the PZ membrane was tested using a series of neutral organic solutions of different molecular sizes:[16] ethyl alcohol (0.4 nm), isopropyl alcohol (IPA; 0.48 nm), *s*-butyl alcohol (~0.54 nm), glucose (0.73 nm) and maltose (0.94 nm). It can be seen that the PZ nanocomposite membrane almost completely (>95 to 99%) rejected neutral molecules larger than 0.73 nm. However, the molecules of less than 0.54 nm, which were a little larger in size than the water, showed only a moderate rejection by the PZ nanocomposite membrane. This was possibly due to the presence of larger pores of the nanocomposite membrane. On the other hand, the PZ nanocomposite membranes that were prepared by the conventional method showed approximately the same permeability properties as the PA membrane (see Fig. S6†), such as a low water flux and a high rejection of an IPA and *s*-butyl alcohol aqueous solution. Based on these results, the use of the Ferry equation (see eqn. S1†) shows the mean "pore" size of the PZ nanocomposite membrane to be approximately 0.79 nm (see Fig. S7†), which corresponds to the pore size of the incorporated zeolite Y (~0.74 nm), whereas the pure polyamide membrane typically consists of a polymer active layer that is dense with interstitial voids (<0.6 nm) between the polymer chains.[8] Thus, this work could provide a promising strategy for control of the pore size of the resultant membrane with intrinsic pores in the incorporated materials.

In conclusion, a new type of polyamide-zeolite nanocomposite membrane with a high performance has been fabricated by a promising "pre-seeding" method without additional additives and post-treatment that can improve the membrane performance. This membrane material, which is based on a zeolite-incorporated thin polyamide membrane, shows a high water flux with no considerable loss of its capacity for salt rejection (>95%). This work promises the development of a better polyamide-zeolite polymer membrane with a good capacity, and is likely to lead to a promising strategy to prepare high-performance organic–inorganic thin polymer membranes for use in water purification. The strategy of pre-arranging the zeolite crystals on the support prior to polymerization allows the designing of a composite membrane morphology in a more robust way. In all, we demonstrate a very simple trick that could be universally used for the preparation of composite top-layers for many types of inorganic-incorporated polymer membranes, not only for separation but also for other applications, such as sensors, optics, *etc*. It could also be useful for other future applications of similar composites, where the transport characteristics of zeolites or similar nanoparticles can add more functionality. In addition, the present study provides a promising strategy to control the pore size of an organic–inorganic polymer membrane with intrinsic pores in the incorporated porous materials.

Notes and references

1 M. Elimelech, *J. Water Supply Res. Technol. Aqua*, 2006, **55**, 3.
2 T. Shintani, H. Matsuyama and N. Kurata, *Desalination*, 2009, **247**, 370; M. E. Suk, A. V. Raghunathan and N. R. Aluru, *Appl. Phys. Lett*., 2008, **92**, 133120.
3 A. Bhattacharya and P. Ghosh, *Rev. Chem. Eng*., 2004, **20**, 111.
4 D. X. Wang, L. Wu, Z. D. Liao, X. L. Wang, Y. Tomi, M. Ando and T. Shintani, *J. Membr. Sci*., 2006, **284**, 384; M. Zhou, P. R. Nemade, X. Lu, X. Zeng, E. S. Hatakeyama, R. D. Noble and D. L. Gin, *J. Am. Chem. Soc*., 2007, **129**, 9574.
5 L. M. Robeson, *J. Membr. Sci*., 1991, **62**, 165; B. D. Freeman, *Macromolecules*, 1999, **32**, 375.
6 W. J. Koros, *AIChE J*., 2004, **50**, 2326; J. K. Holt, H. G. Park, Y. M. Wang, M. Stadermann, A. B. Artyukhin, C. P. Grigoropoulos, A. Noy and O. Bakajin, *Science*, 2006, **312**,

1034; P. Rittigstein, R. D. Priestley, L. J. Broadbelt and J. M. Torkelson, *Nat. Mater.*, 2007, **6**, 278; T. C. Merkel, B. D. Freeman, R. J. Spontak, Z. He, I. Pinnau, P. Meakin and A. J. Hill, *Science*, 2002, **296**, 519.
7 D. S. Sholl and J. K. Johnson, *Science*, 2006, **312**, 1003; P. S. Tin, T. S. Chung, L. Y. Jiang and S. Kulprathipanja, *Carbon*, 2005, **43**, 2025.
8 G. L. Jadav and P. S. Singh, *J. Membr. Sci.*, 2009, **328**, 257; H. S. Lee, S. J. Im, J. H. Kim, H. J. Kim, J. P. Kim and B. R. Min, *Desalination*, 2008, **219**, 48; M. L. Lind, A. K. Ghosh, A. Jawor, X. Huang, W. Hou, Y. Yang and E. M. V. Hoek, *Langmuir*, 2009, **25**, 10139.
9 W. J. Koros and R. Mahajan, *J. Membr. Sci.*, 2000, **175**, 181.
10 H. Dobbs and D. Bonn, *Langmuir*, 2001, **17**, 4674.
11 S. H. Kim, E. Y. Kwak and T. Suzuki, *Environ. Sci. Technol.*, 2005, **39**, 1764.
12 M. L. Lind, B. H. Jeong, A. Subramani, X. Huang and E. M. V. Hoek, *J. Mater. Res.*, 2009, **24**, 1624; B. H. Jeong, E. M. V. Hoek, Y. Yan, A. Subramani, X. Huang, G. Hurwitz, A. K. Ghosh and A. Jawor, *J. Membr. Sci.*, 2007, **294**, 1.
13 V. Freger, *Langmuir*, 2005, **21**, 1884.
14 L. J. Bellamy, *The Infra-Red Spectra of Complex Molecules*, Chapman and Hall Ltd., London, 1975.
15 T. Tsuru, M. Urairi, S. I. Nakao and S. J. Kimura, *J. Chem. Eng. Jpn.*, 1991, **24**, 518.
16 X. Wang, T. Tsuru, S. Nakao and S. Kimura, *J. Membr. Sci.*, 1997, **135**, 19.

